THE BAND-PASS DISTRIBUTED AMPLIFIER

By V. C. Rideout and T. P. Tung
(*University of Wisconsin*)

Abstract

General expressions have been obtained for the gain of a simple distributed amplifier with any number of tubes joined by identical reactive symmetrical filter sections, with or without unsymmetrical terminating sections at the ends of the filter chains. These results may be applied to the band-pass as well as to the low-pass distributed amplifier. It is shown that reduction of band-edge peaks is much more difficult of accomplishment in the band-pass case. Some considerations regarding the choice of the most suitable filter network in the band-pass case are given, as well as experimental results.

I. Introduction

The wide bands of frequency which must be amplified in many modern communication systems have aroused interest in several new types of wide-band amplifiers. Among these is the *travelling-wave* amplifier,[1] which uses an helix and an axial stream of electrons and may be used down to frequencies as low as 200 mc. Low-pass forms of the *distributed amplifier*, invented by Percival[2] in 1935 have been described by Ginzton,[3] Rudenberg[4] and others.[5] This type of amplifier, which uses orthodox tetrodes or pentodes separated by filter sections may also be built in band-pass form. This paper is chiefly concerned with these band-pass forms, although the general expressions obtained for gain in Appendices A and B may be used for the low-pass case as well.

II. Simple Gain Expressions

Since we are primarily interested in the band-pass case it is useful to develop simple formulas from the transformer-coupled amplifier. These apply in the case of other kinds of filter sections, but only the transformer permits free choice of load and generator impedances.

In the circuit of Fig. 1 (*a*), with transformers designed to match the generator and load impedances to the grid and plate loading resistors the mid-band power gain is,[6, 7]

$$G_0 = \frac{g_m{}^2 R_g R_p}{4} = \frac{g_m}{4\,C_p C_g}\left(\frac{1}{2\pi\Delta f}\right)^2 \tag{1}$$

Here Δf is the bandwidth between cut-off points of the transformers viewed as filter sections. (Δf is approximately the bandwidth to points two *db* down on the transmission curve). Simple parallel or push-pull parallel combinations of

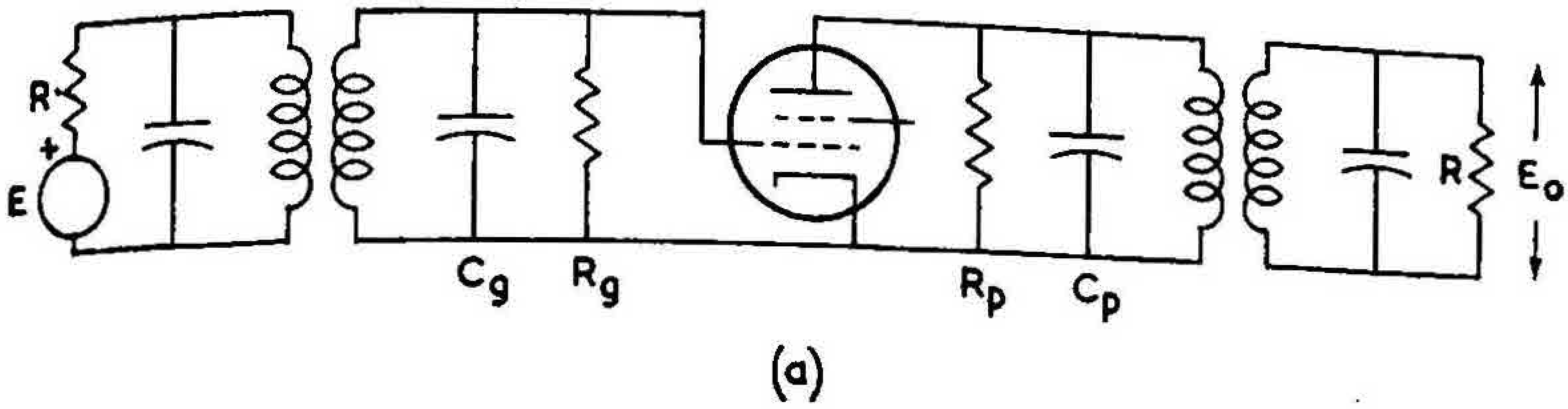

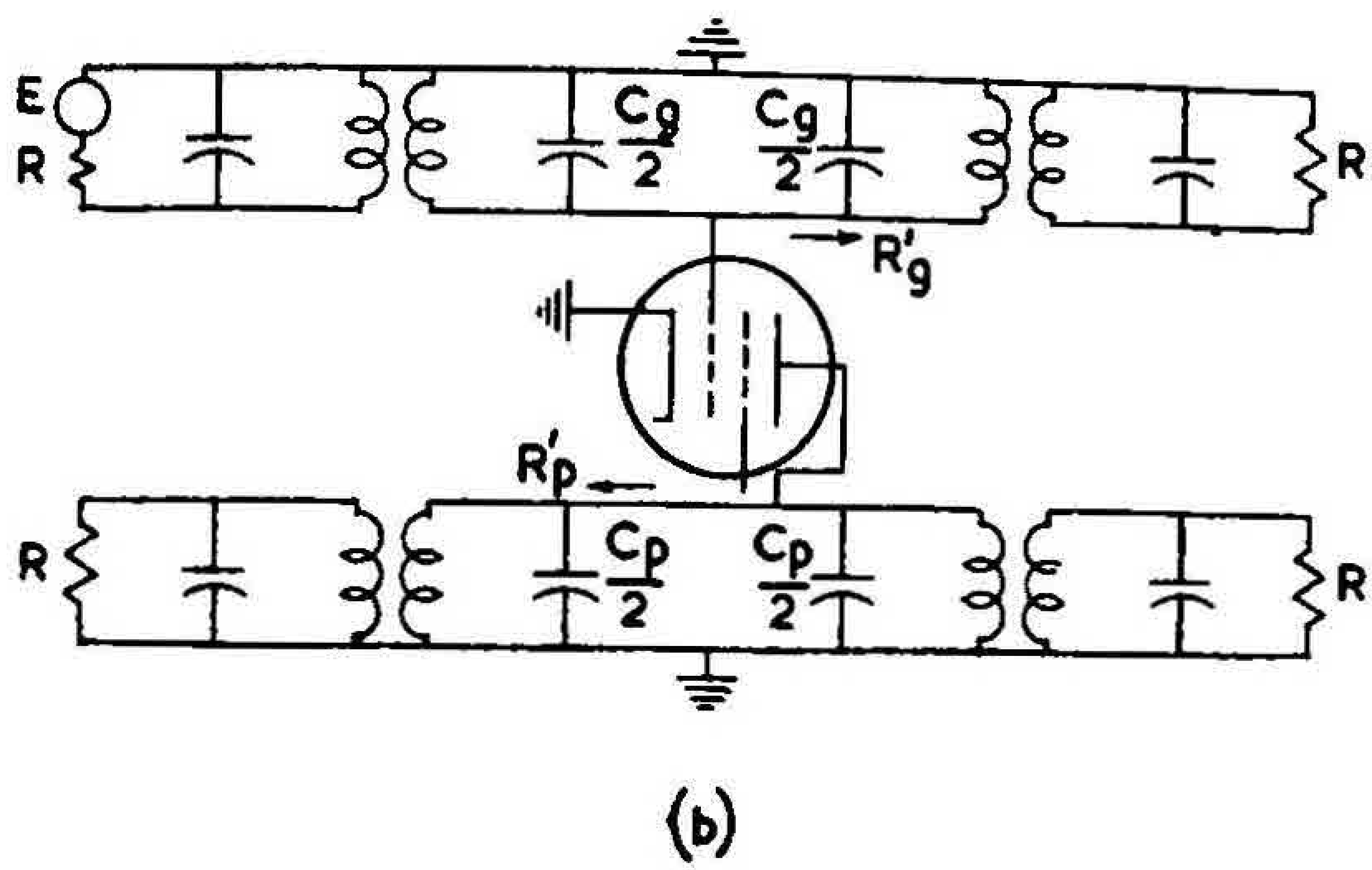

FIG. 1. (*a*) Single-stage transformer-coupled amplifier used as standard reference amplifier. (*b*) An increase in gain of 6 *db* is possible by capacitance splitting.

tubes increase both the transconductance g_m and the capacitance so that no increase in gain results for a given bandwidth.

If the input and output capacitances are split between two transformers, as shown in Fig. 1 (*b*), the impedance levels will be doubled, and the mid-band gain will increase to $4\,G_0$, or 6 *db* above that of the reference amplifier in Fig. 1 (*a*).

If $2n$ transformers (n in each line) are used to couple $n-1$ tubes, as shown in the distributed amplifier of Fig. 2, the transconductance will be effectively

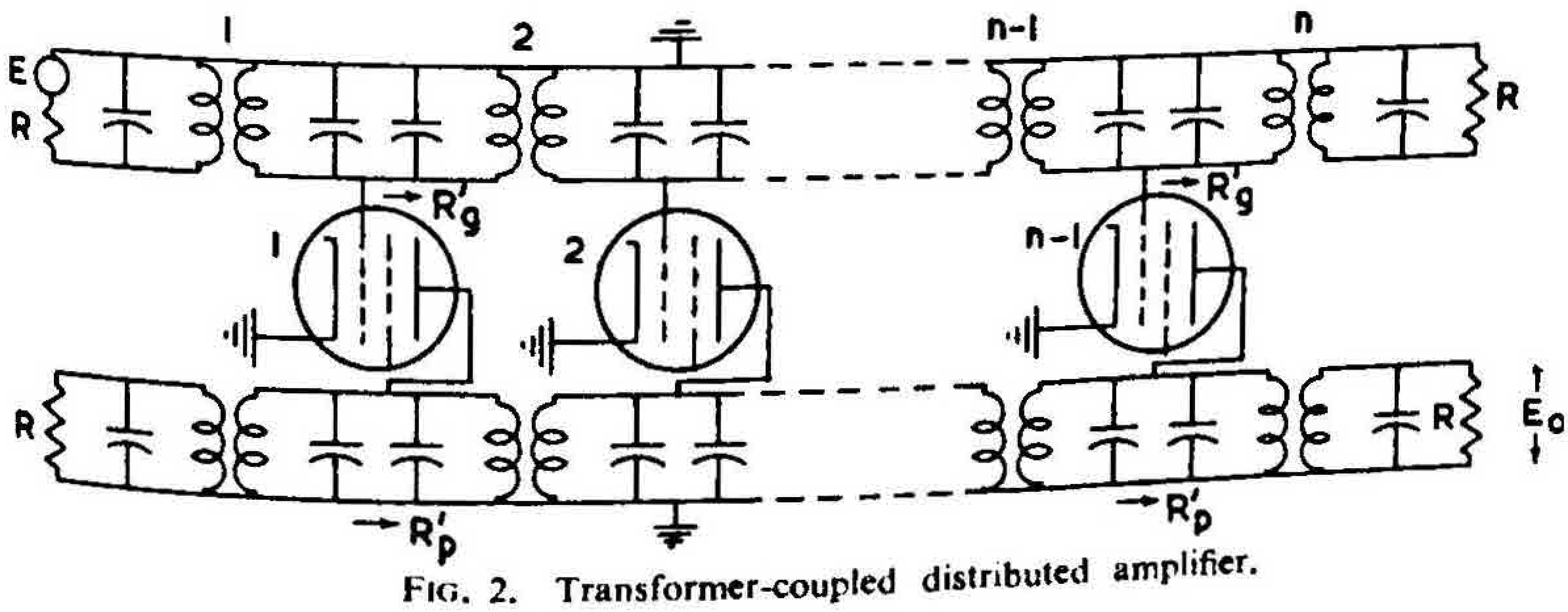

FIG. 2. Transformer-coupled distributed amplifier.

$(n-1)$ times greater, and the gain will be increased by $4(n-1)^2$ times that of the reference amplifier. Thus this amplifier has an advantage over the reference amplifier of 6 *db* from capacitance splitting and $20 \log (n-1)$ *db* for the $(n-1)$ tubes, or

$$G_{n-1} = [G_0 + 6 + 20 \log (n-1)]\ db. \tag{2}$$

The bandwidth, assuming all transformers to have the same cut-off frequencies, will roughly correspond to the bandwidth between these frequencies.

III. THE DISTRIBUTED AMPLIFIER

General expressions for gain have been obtained for the distributed amplifier of Fig. 3, in Appendix A. The amplifier contains $n-1$ identical tubes which give negligible resistive loading on the grid and plate lines, and which are coupled as

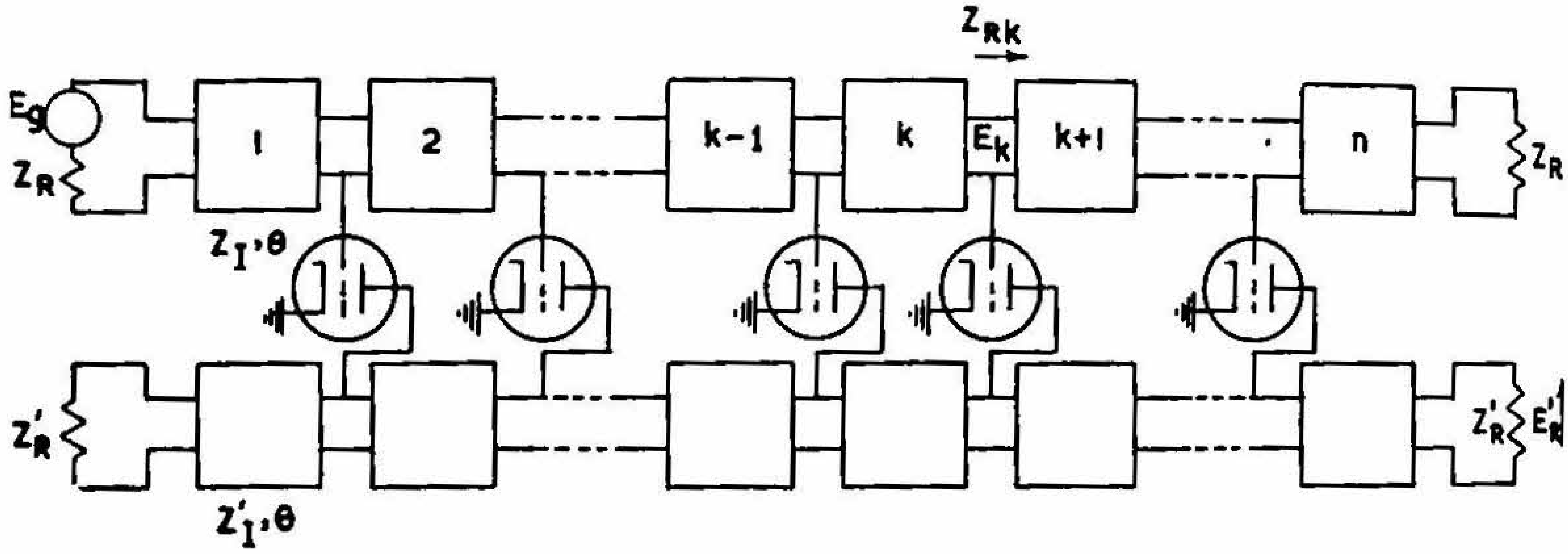

FIG. 3. Distributed amplifier with $2n$ identical filter sections.

shown by $2n$ reversible filter sections, each with propagation function θ. The input and output capacitances of the tubes are included in the filters. The grid chain has n sections of characteristic impedance $\mathbf{Z}_I$ and is terminated in $\mathbf{Z}_R$. The corresponding impedances for the plate chain are $\mathbf{Z}_I'$, $\mathbf{Z}_R'$. The characteristic impedances, normalized with respect to the terminating impedances are assumed to be equal for each chain,

$$\mathbf{z} = \frac{\mathbf{Z}_I}{\mathbf{Z}_R} = \frac{\mathbf{Z}_I'}{\mathbf{Z}_R'}. \tag{3}$$

The gain, at frequencies where $\mathbf{z} = 1$ (usually at midband), may be obtained from (1) by using a transconductance increased by $(n-1)$ times and by using, in place of R_g and R_p, the impedances $\mathbf{Z}_R$ and $\mathbf{Z}_R'$. (The latter are twice the value of R_g and R_p for the same bandwidth and are assumed to be resistive.)

$$G_0 = \frac{\mathbf{E}_R'^2}{\mathbf{Z}_R'} \times \frac{4\mathbf{Z}_R}{\mathbf{E}_g^2} = \frac{g_m \mathbf{Z}_R \mathbf{Z}_R'}{4} (n-1)^2. \tag{4}$$

The forward voltage gain, taken as the ratio of output voltage to internal generator voltage is therefore, where $\mathbf{z} = 1$,

$$A_{f_0} = \frac{E_R'}{E_g} = \frac{g_m Z_R Z_R' (n-1)}{4}. \tag{5}$$

The general expression for forward gain, normalized to unity where $z = 1$ by dividing the actual voltage gain by A_{f_0} is, from (15) App. A,

$$A_f = 2z^2 \frac{[(1+z^2)\cosh n\theta + 2z\sinh n\theta] + (1-z^2)\dfrac{\sinh(n-1)\theta}{(n-1)\sinh\theta}}{[(1+z^2)\sinh n\theta + 2z\cosh n\theta]^2}. \tag{6}$$

The backward gain to the plate chain terminal at the left in Fig. 3 is, from (16) App. A,

$$A_b = 2z^2 \frac{\dfrac{\sinh(n-1)\theta}{(n-1)\sinh\theta}[(1+z^2)\cosh n\theta + 2z\sinh n\theta] + (1-z^2)}{[(1+z^2)\sinh n\theta + 2z\cosh n\theta]^2}. \tag{7}$$

If the grid and plate lines are terminated in their image impedances, $Z_R = Z_I$, $Z_R' = Z_I'$, $z = 1$ (all frequencies), then from (6) and (7),

$$A_f = \epsilon^{-n\theta}, \tag{8}$$

$$A_b = \frac{\sinh(n-1)\theta}{(n-1)\sinh\theta}\,\epsilon^{-n\theta}. \tag{9}$$

If terminating filter sections are added on at the ends of the n-section filter chains, new general expressions for gain can be obtained as shown in Appendix B, Equations (6) and (7). These are identical with those in (6) and (7) above, except for the multiplying factor $z_{01}z_{02}/(z_{01}\cosh\phi + \sinh\phi)^2$, and the substitution of $n+1$ for $n-1$, which is made because two more tubes can now be added. The impedances z_{01} and z_{02} are the image impedances of the terminating networks, in this case normalized with respect to the impedance offered by the terminating section.

IV. The Problem of Band-Edge Peaks and Ripples

Fig. 4 shows a distributed amplifier with terminating sections with sketches in each block to indicate the variation of characteristic impedance with frequency

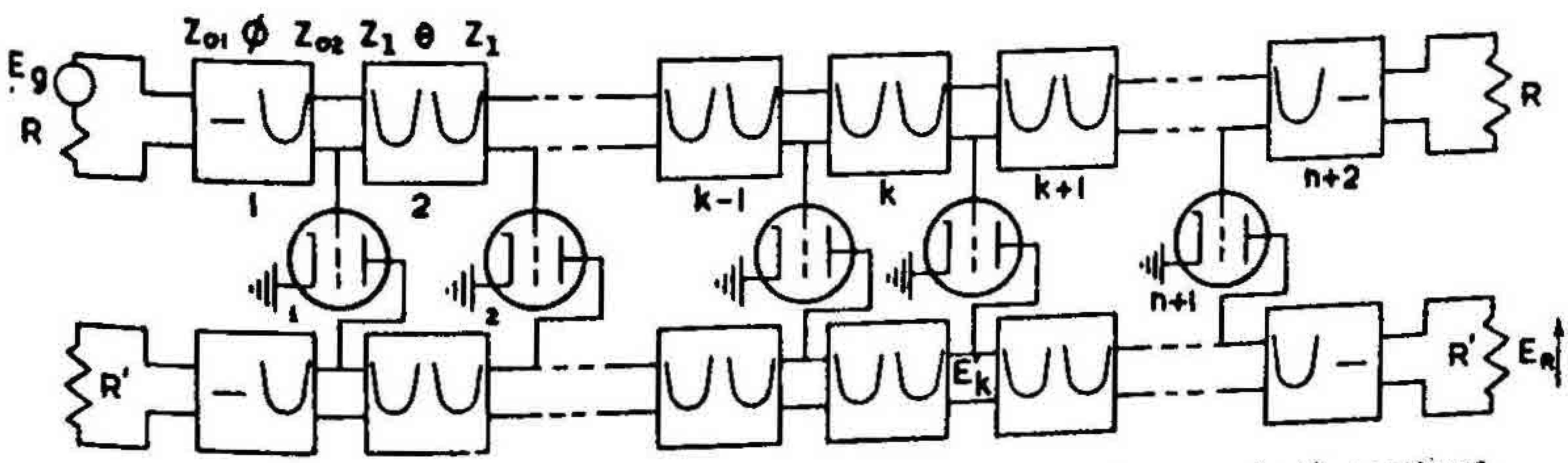

FIG. 4. The distributed amplifier of Fig. 4 with the addition of four terminating sections and two tubes.

within the pass-band. If these sections are of proper design (and complexity) to match the filter chain to the resistive impedances outside, as shown in Fig. 4, and if all internal characteristic impedances are characteristically U-shaped as shown, we can show that a band peaked at the edges may still be expected. For if $\mathbf{z}_{01} = 1$, $\mathbf{z} = 1$ then expressions for normalized gain in App. B reduce to,

$$\mathbf{A}_f = \mathbf{z}_{02}\epsilon^{-(n\theta+2\phi)}, \tag{10}$$

$$\mathbf{A}_b = \frac{\sinh (n+1)\,\theta}{(n+1)\sinh\theta}\,\mathbf{z}_{02}\,\epsilon^{-(n\theta+2\phi)}. \tag{11}$$

In the pass-band $\theta = j\beta$, $\phi = j\beta'$ and,

$$\mathbf{A}_f = \mathbf{z}_{02}\,\epsilon^{-j(n\beta+2\beta')}, \tag{12}$$

$$\mathbf{A}_b = \frac{\sinh (n+1)\,\beta}{(n+1)\sin\beta}\,\mathbf{z}_{02}\epsilon^{j-(n\beta-+2\beta')}. \tag{13}$$

Thus for a perfectly matched amplifier the overall gain characteristic follows the same curve as the image impedance $\mathbf{Z}_{02}$ of the terminating network. In the case of simple filters with U-shaped curves for $\mathbf{Z}_{02}$ and $\mathbf{Z}_I$ as shown in Fig. 4 a band peaked at the edges will result; thus simple terminating sections remove ripples, but not peaks, in the band characteristic. If $\mathbf{Z}_{02}$ were constant the forward gain characteristic would be straight and uniform throughout the band, and the backwards gain would follow a typical $\sin (n+1)\,\beta/(n+1)\sin\beta$ curve.

Unfortunately a constant $\mathbf{Z}_{02}$ over the whole pass-band is impossible of attainment. This may be proved as follows. In a reactive four-terminal network the open and short-circuit impedances are purely reactive, so that the image impedances are,

$$Z_I' = \sqrt{jX_{oc1}\cdot jX_{sc1}},\quad Z_{I2} = \sqrt{jX_{oc1}\cdot jX_{sc2}}. \tag{14}$$

The propagation function is,

$$\theta = \alpha + j\beta = \tfrac{1}{2}\ln\frac{\sqrt{\dfrac{X_{oc1}}{X_{sc1}}}+1}{\sqrt{\dfrac{X_{oc2}}{X_{sc2}}}-1}. \tag{15}$$

Within the pass-band $\alpha = 0$ and the image impedances are real and therefore the open and short circuit reactances must be of opposite sign. At the edges of the pass-band one or the other, but not both of these reactances must change sign. By Foster's reactance theorem the slopes of these reactance curves *versus* frequency are always positive so they must pass through zero or infinity to change sign. The image impedances must therefore be either zero or infinity at the edges of the pass-band. In the case at hand, of filters with capacitive input, the image impedances will be infinite at the edges of the pass-band, and the gain of a distributed amplifier with perfect terminating sections will theoretically approach infinity there. In practice the use of ordinary terminating sections and the presence of dissipation will limit the gain at the band edges to some finite value, but serious peaks can always be expected.

The problem of controlling these peaks at the band-edges has been recognized as a serious one and several methods of compensation have been proposed. One method is to pair the plates, or connect them together at alternate points along the filter, inserting dummy capacitances elsewhere. This method has the disadvantage that the plate line capacitance are doubled, thus halving plate line impedance at a cost of 6 *db* in gain, in the band-pass case.

Another method for flattening the high-frequency peak in a low-pass distributed amplifier uses negative mutual inductance to give the equivalent of m-derived sections with m greater than unity. A third method uses a bridged-tee structure. These two methods are not applicable to the band-pass case, because their conversion to band-pass form would require negative capacitances. A fourth method for controlling band-edge peaking is by the use of two lines of tubes with separate interstages between individual pairs of tubes, as shown in Fig. 5. These interstages may easily be designed to correct for peaking. However the number

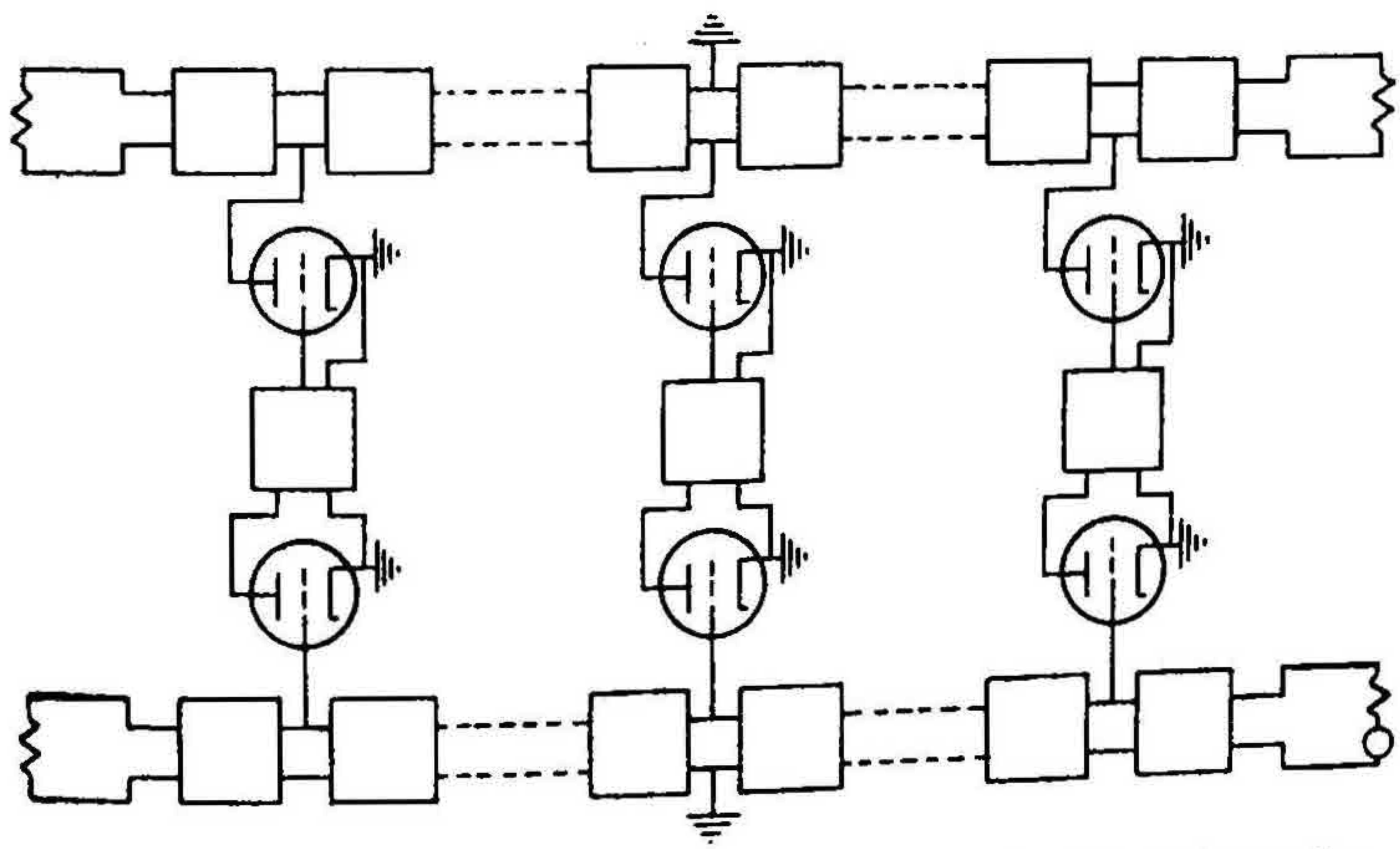

FIG. 5. Block diagram showing a scheme for securing a flat band by peak-correcting in individual interstages between two lines of tubes.

of tubes is doubled, with small gain advantage, or even with a loss in gain, depending on the bandwidth required.

A practical solution for the band-pass design in the case where very wide bands are desired is to build a low-pass amplifier with a low-frequency cut-off determined by the coupling capacitors. Then only the high-frequency peak needs to be contended with, and if it is at a high enough frequency[4] so that appreciable grid loading occurs it may be flattened by this effect. There is some loss in efficiency if an appreciable part of the band must be thrown away. In the band-pass amplifiers described below the peaks and ripples were minimized by the use of double-tuned transformers as filter sections and series-parallel transformers as terminating sections, as explained in the following section. It was found experimentally that further reduction of peaks was possible in amplifiers containing up to four tubes by slightly detuning the filter lines.

V. Choice of Filter Sections in a Band-Pass Distributed Amplifier

The simplest choice for a band-pass filter section which would include the shunt capacitance in the tubes is either the band-pass constant-k or the parallel-tuned transformer, a filter which has no low-pass counterpart. In App. C it is shown that the parallel-tuned transformer has the same characteristic impedance as the constant-k filter (mid-shunt), but only half the propagation function. This difference might be expected because in π form the parallel-tuned transformer has one less reactive element.

Peaks at the edges of the band might be expected in either case if simple resistive terminations are used as well as ripples near the edge of the band. Calculations show that in particular cases the peaks are lower in the parallel-tuned transformer case, though no general expression has been obtained.

The ripple appearing in the gain characteristic may be approximately determined by a consideration of the equation for forward gain in the case where terminating sections are not used. Within the pass-band the normalized power gain may be shown to be, from (6),

$$G_f = A_f^2 = z^4 \left[\frac{4z^2 + (1-z^2)^2 \cos^2 n\beta + 2(1-z^4)\dfrac{\sin(n-1)\beta \cos n\beta}{(n-1)\sin\beta} + \dfrac{\sin^2(n-1)\beta}{(n-1)^2 \sin^2\beta}(1-z^2)^2}{4z^2 + (1-z^2)\sin^2 n\beta} \right]. \tag{16}$$

If n is large the third and fourth terms in the numerator may be neglected. The remaining terms in $\sin^2 n\beta$ and $\cos^2 n\beta$ will combine to give ripples near the edge of the band where z begins to differ appreciably from unity. The variation in gain will be approximately of the order of the square of the following:

$$G = \frac{1}{1+(\frac{1}{4})(z - 1/z)^2 \sin^2 n\beta} = \frac{4z^2}{4z^2 + (1-z^2)^2 \sin^2 n\beta}, \tag{17}$$

which is, incidentally, just the transmission loss of an n-section filter.[8]

A comparison of the transmission gain G for five-section filters of the constant-k and double-tuned transformer types was made to illustrate the relative ripple amplitudes to be expected in distributed amplifiers using these sections. The

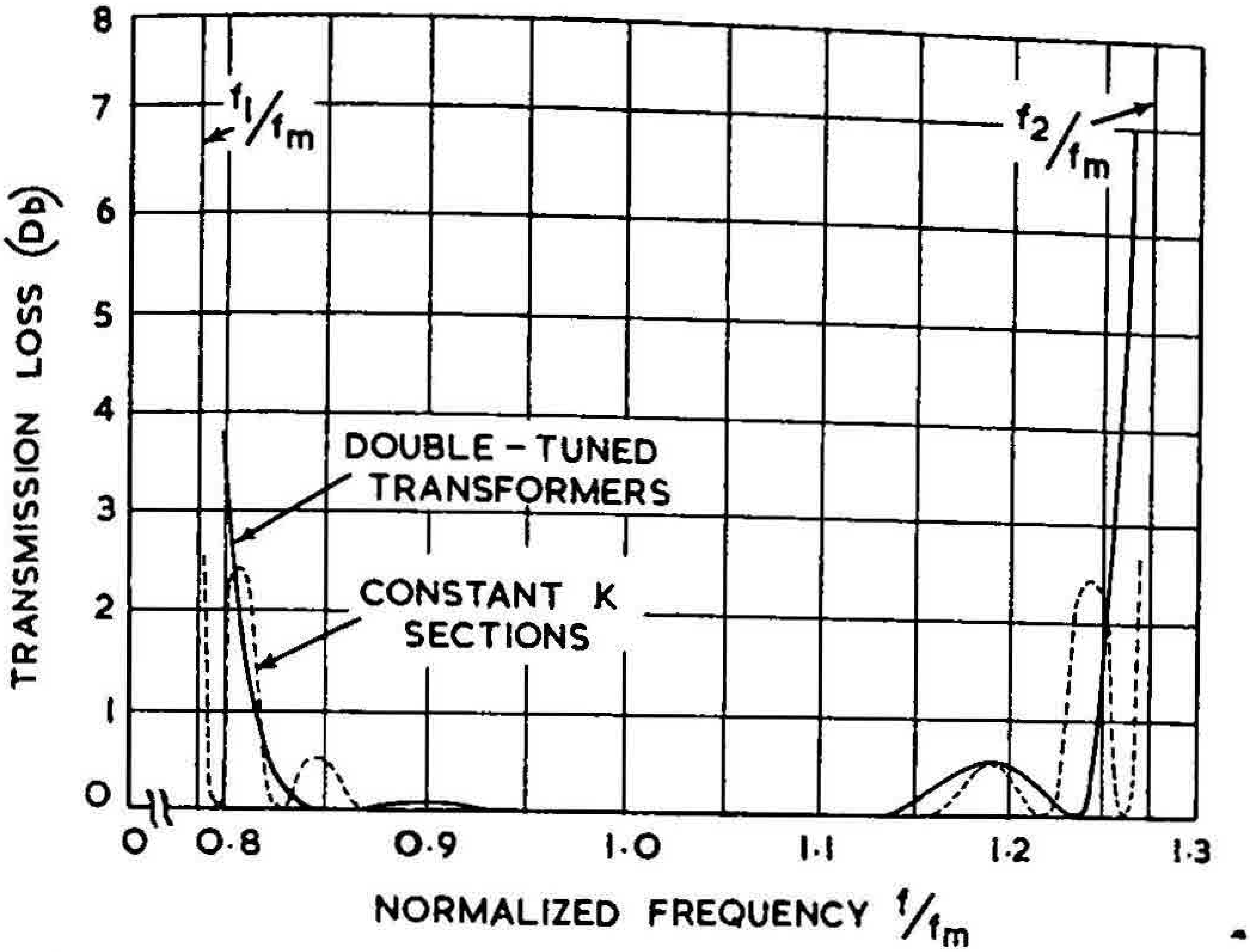

FIG. 6. Transmission loss for five double-tuned transformers in tandem compared with that for five band-pass constant-k sections.

calculated values of transmission loss, ($L = 1/G$), are shown in Fig. 6, and the lower ripple amplitudes of the transformer filter sections is quite apparent. With this advantage, as we have stated, goes some reduction in the peaks. Thus, of the two simplest filter sections available, the tuned transformer is considerably superior.

One advantage which the band-pass distributed amplifier possesses over the low-pass amplifier is that transformers can be used as terminating sections to transform the impedance in the filter line, which is fixed by bandwidth requirements, to the value required by coaxial line or other impedances. This impedance ratio will often be such that if the parallel-tuned transformer is used for end sections, equivalent π or T structures cannot be used and sometimes even mutual coupling is not practically possible. In this case series-parallel tuned transformers may be used. Design formulas for this case are developed in Appendix 4, based on the equivalence between this transformer and a constant-k band-pass half-section. Therefore, because the parallel-tuned transformer has the same image impedance as the mid-shunt image impedance in the constant-k section, the series-parallel transformer (shunt capacitance side) may be exactly matched to the parallel-tuned transformer, simply by making the cut-off frequencies the same.

VI. Experimental Results

A number of experimental amplifiers, low-pass as well as band-pass were built. In the low-pass amplifiers large (150 mmf.) capacitors were shunted across the input and output of each tube so that neither gain nor bandwidth would be

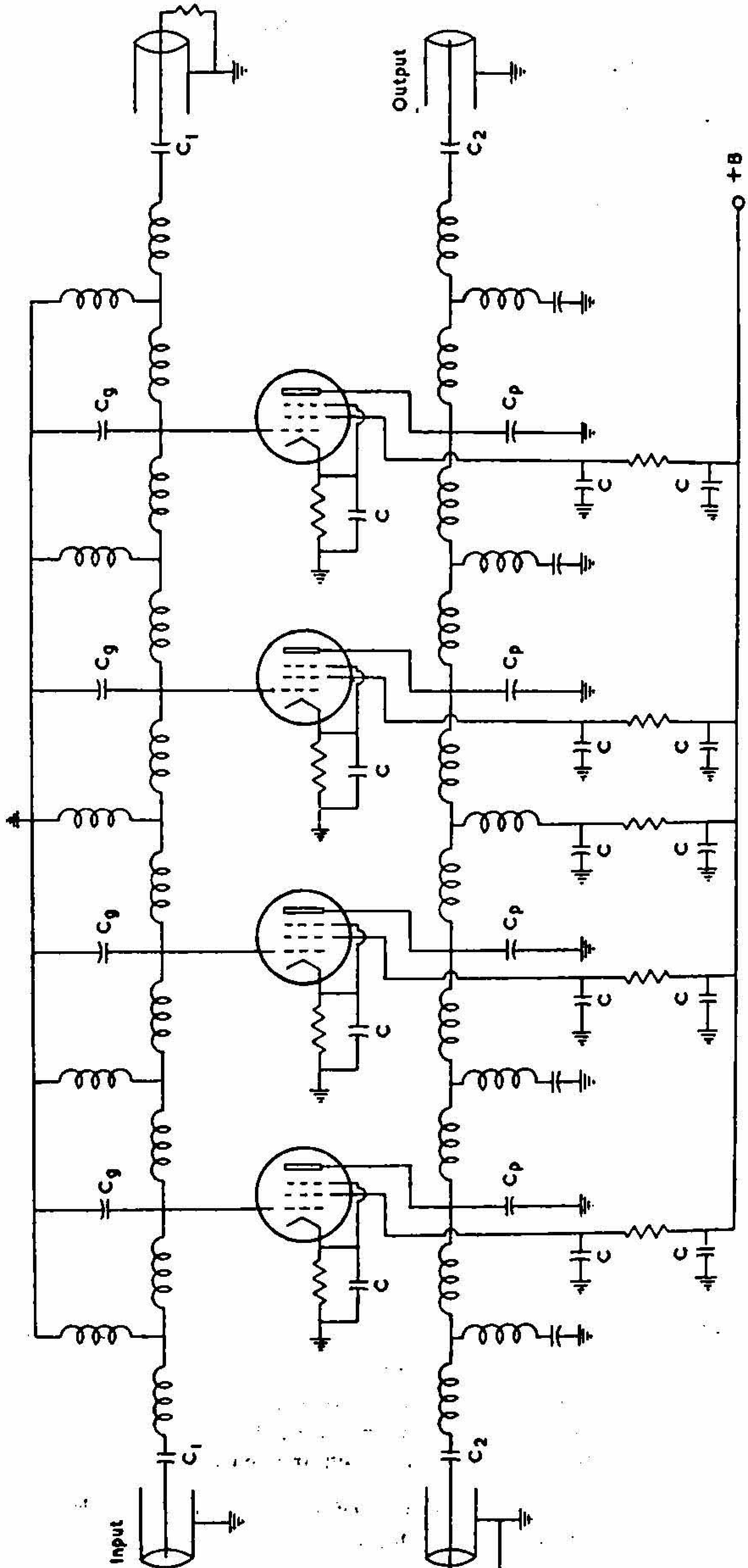

FIG. 7. Circuit diagram for a four-tube band-pass distributed amplifier.

too large for accurate measurement. These low-pass amplifiers were used to check the theoretical expressions developed in this paper.

A band-pass amplifier (Fig. 7) was built with a center frequency of 65 mc. using 6*AK*5 tubes selected for nearly identical transconductance and shunt capa-

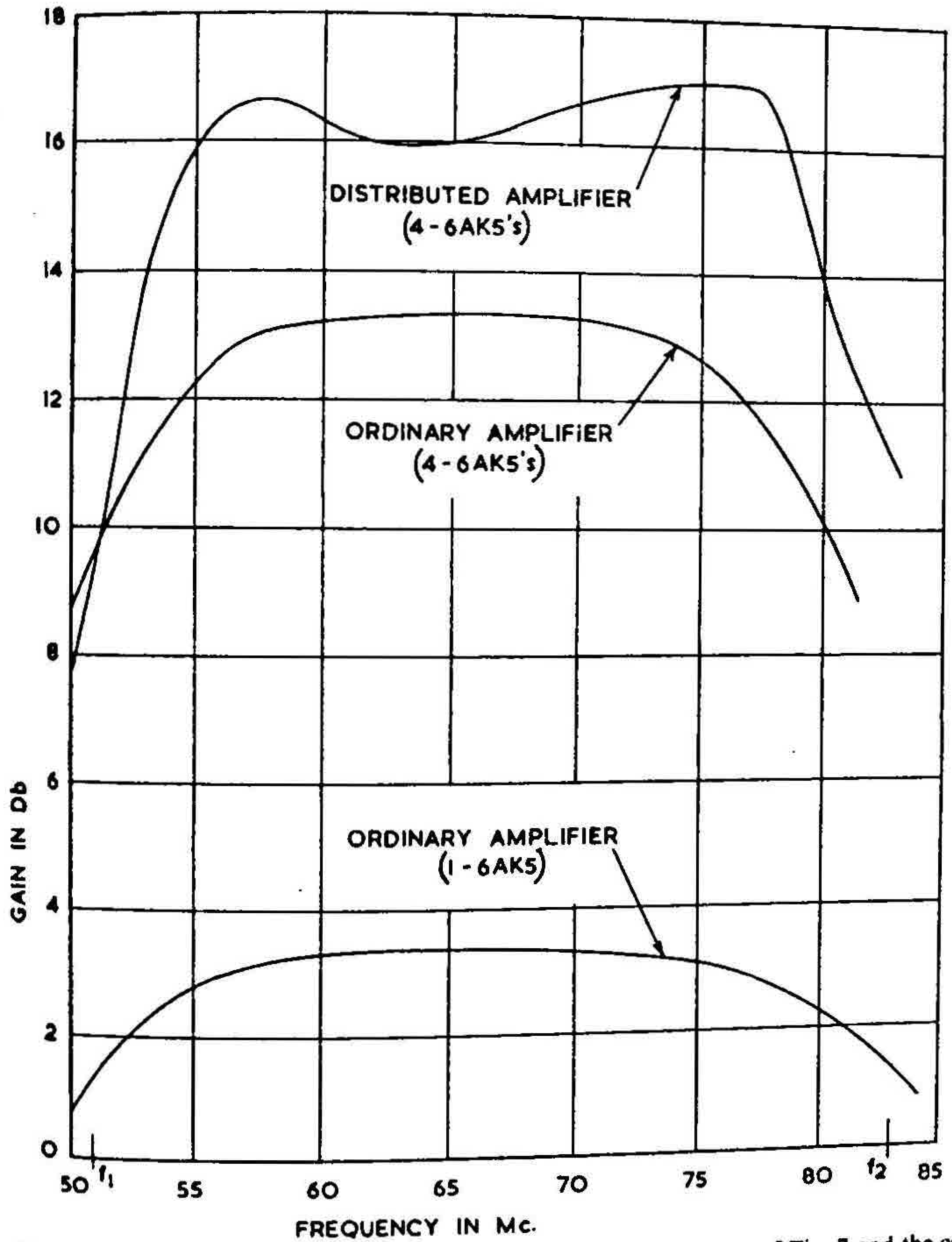

Fig. 8. Comparison of the measured gain characteristic of amplifier of Fig. 7 and the calculated gain for a single-tube and for a four-tube amplifier using the same tubes and matched transformers with the same cut-off frequencies.

citance. Parallel-tuned transformers were used as filter sections, with series-parallel transformers at the ends of the filter chains to match them to the 51-ohm.

impedance used in the measuring equipment. In this amplifier great care was taken to provide good shielding and adequate by-passing. Transformers were built in equivalent-T form to avoid difficulties involved in working with mutual impedances.

A value of 0·45 was chosen for the coupling coefficient k of the parallel-tuned transformer giving (Eq. C-10) cut-off frequencies at 51 mc. and 82·8 mc., a bandwidth to mid-frequency ratio of 0·49. The mid-band gain expected can be determined by first calculating the gain of a single tube amplifier of the same bandwidth. The effective input and output capacities and average transconductances of the tubes used were $C_g = 8 \cdot 3\,\mu\mu f$, $C_p = 6 \cdot 0\,\mu\mu f$, $g_m = 4030\,\mu$mhos. The calculated single-stage mid-band gain is, from (1), $G_0 = 3 \cdot 1$ *db*. The mid-band gain expected in the four tube distributed amplifier is, from (2), $G_0 = 3 \cdot 1 + 6 + 20 \log 4 = 21 \cdot 1$ *db*. The experimental curve shown in Fig. 8 shows that this figure was not reached by about 5 *db*. This may be partly accounted for by loss in the filter elements, and by grid and plate loading. Ripples and band-edge peaks were reduced by slight detuning of trimmer condensers, while the band was observed with the aid of a sweeping oscillator.

Note that the gain is higher than that calculated for an ordinary amplifier with the same cut-off frequencies and with four *6AK5* tubes in tandem, with matched transformers. Such a tandem amplifier can be increased in gain theoretically by 9 *db* by the use of mismatched interstage transformers. The advantage of the distributed amplifier becomes apparent if the effect of doubling the bandwidth is considered. This will cause the gain of the distributed amplifier or the ordinary single-stage amplifier to drop by 6 *db*, but the four-tube amplifier with the ordinary tandem connection will drop in gain by four times as much, or 24 *db*.

A similar amplifier using four tubes but with the two middle tubes in parallel was built by the senior author at the Bell Telephone Laboratories in 1946, and gave similar results, but was considerably easier to adjust for a flat band, because there were fewer filter sections per chain. The band-pass characteristic for this amplifier is shown in Fig. 9. It will be noted that the band shape of the distributed amplifier is very similar to that calculated for a single tube amplifier although it had 8 transformers rather than 2, and about 9·5 *db* more gain. The delay curve was measured for this amplifier and was also very close to that calculated for the single tube amplifier (neglecting the fixed delay which is one of the great disadvantages of the distributed amplifier).

One important advantage expected in these amplifiers is an increase in power-handling capacity. One measure of this is the power at which the gain is reduced by some given amount. An appreciable gain reduction or compression occurs at a power where the peak plate current swing approaches the d-c plate current. It would be expected that the increased power output for a distributed amplifier would be 3 *db* (because of output impedance increase with capacitance splitting)

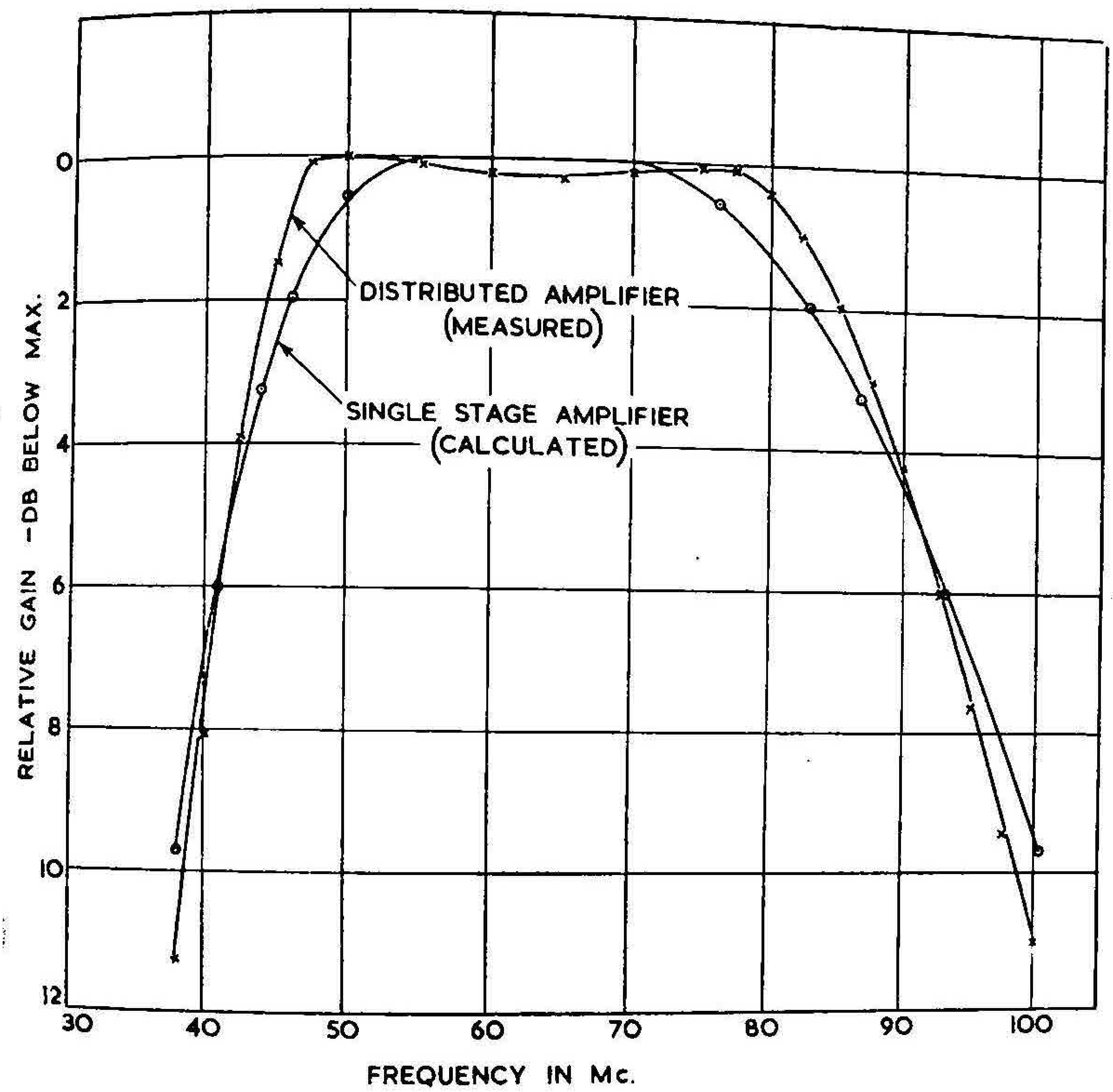

FIG. 9. Measured band shape for a four-tube distributed amplifier (two middle tubes in parallel) compared to calculated single-tube amplifier band shape.

plus 20 log (n — 1), (for the n — 1 tubes) over a single-tube amplifier with matched transformer output. The expected advantage of 15 *db* in the four tube 6*AK*5 amplifier was not obtained in practice, the measured value being 7½ *db*. The reasons for this discrepancy have not been fully investigated.

Another advantage expected in the wave-amplifier is an improvement in noise Fig. 3. The measured noise figure for the four-tube 6*AK*5 amplifier was 6 *db*, which is appreciably better than may be expected from an amplifier of the same bandwidth using single 6*AK*5 tubes in tandem, and with matched input.

REFERENCES

1. Pierce, J. R. .. "Travelling-Wave Tubes," *B.S.T.J.*, 1950, 29, 1.
2. Percival, W. S. .. *British Patent*, 460, 562, 1935–37.
3. Ginzton, E. L. *et al.* .. "Distributed Amplification," *Proc. I.R.E.*, 1948, 36, 956.

4. Rudenberg, H. G. and Fitzroy Kennedy "200 Mc. Travelling-Wave Chain Amplifier," *Electronics*, 1949, **22**, 106.

5. Wheeler, H. A. .. "Wide Band Amplifiers for Television," *Proc. I.R.E.*, 1939, **27**, 429.

6. Rideout, V. C. . "A Note on a Parallel Tuned Transformer Design," *B.S.T.J.*, 1948, **27**, 96.

7. ——————. .. Unpublished Class Notes.

8. Ragan, G. L. .. *Microwave Transmission Circuits*, McGraw-Hill Book Co., New York, 1948.

9. Guillemin, E. A. .. *Communication Networks*, John Wiley & Sons, New York, 1935, **2**, 151–56.

10. Sandeman, E. K. . "Coupling Circuits as Band-Pass Filters," *Wireless Engineer*, 1941, **18**, 361.

APPENDIX A

In the circuit shown in Fig. 3 the blocks represent image-connected reversible filter sections, each with propagation constant θ. The grid sections have image impedance Z_I, the plate sections Z_I'.

Considering first the grid line, the impedance looking towards the right at the input to the $(k+1)$th section is,

$$Z_{Rk} = Z_I \frac{Z_R \cosh (n-k)\,\theta + Z_I \sinh (n-k)\,\theta}{Z_I \cosh (n-k)\,\theta + Z_R \sinh (n-k)\,\theta}. \tag{A-1}$$

The matrix describing the first k sections of grid line is:

$$\begin{bmatrix} A_k & B_k \\ C_k & D_k \end{bmatrix} = \begin{bmatrix} 1 & Z_R \\ C & 1 \end{bmatrix} \begin{bmatrix} \cosh\theta & Z_I \sinh\theta \\ \frac{1}{Z_I}\sinh\theta & \cosh\theta \end{bmatrix}^k \begin{bmatrix} 1 & 0 \\ \frac{1}{Z_{Rk}} & 1 \end{bmatrix}. \tag{A-2}$$

From (A-2)

$$A_k = \frac{1}{Z_I}(Z_I \cosh k\theta + Z_R \sinh k\theta) + \frac{1}{Z_{Rk}}(Z_I \sinh k\theta + Z_R \cosh k\theta). \tag{A-3}$$

From (A-1) and (A-3),

$$A_k = \frac{Z_I^2 \sinh n\theta + Z_R^2 \sinh n\theta + 2Z_R Z_I \cosh n\theta}{Z_I\,[Z_R \cosh (n-k)\,\theta + Z_I \sinh (n-k)\,\theta]}, \tag{A-4}$$

$$E_k = \frac{E_g}{A_k} = E_g \frac{z_I \cosh (n-k)\,\theta + z_I^2 \sinh (n-k)\,\theta}{(1+z_I^2)\sinh n\theta + 2z_I \cosh n\theta}, \tag{A-5}$$

where $z_I = Z_I/Z_R$ is the normalized image impedance.

Each plate may be considered to be a constant current generator driving two transmission chains as shown for the kth tube in Fig. A-1.

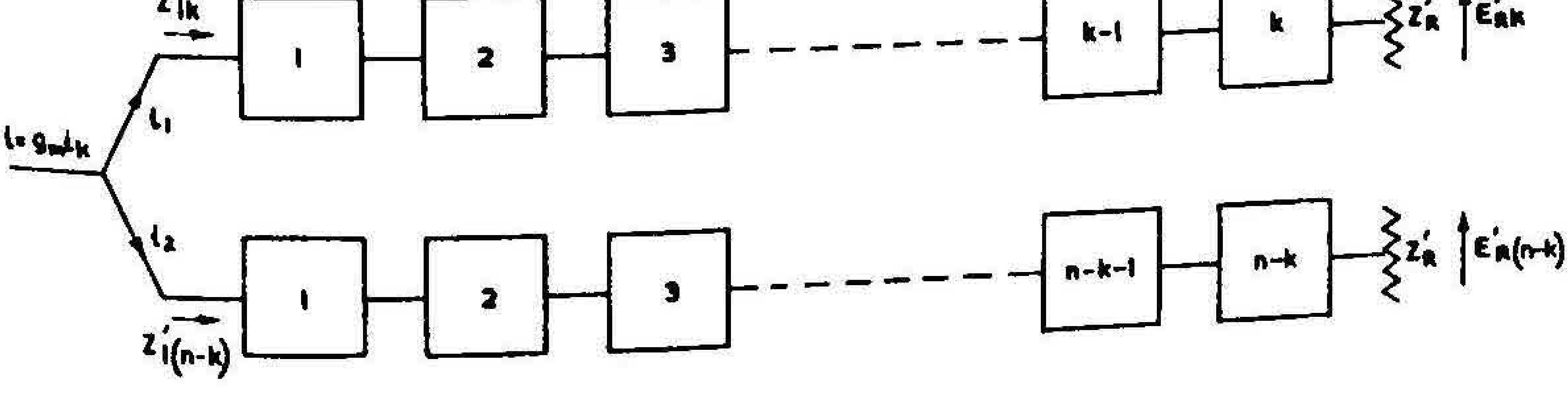

FIG. A-1

The matrix describing the behaviour of the upper chain is,

$$\begin{bmatrix} A_k' & B_k' \\ C_k' & D_k' \end{bmatrix} \doteq \begin{bmatrix} \cosh k\theta & Z_I' \sinh k\theta \\ \frac{\sinh k\theta}{Z_I'} & \cosh k\theta \end{bmatrix} \begin{bmatrix} 1 & 0 \\ \frac{1}{Z_R'} & 1 \end{bmatrix}. \tag{A-6}$$

From (A-6)

$$E_{Rk} = \frac{i_1}{C_k'} = \frac{Z_I' Z_R' i_1'}{Z_I' \cosh k\theta + Z_R' \sinh k\theta}$$

$$= \frac{Z_I' Z_R'}{Z_I' \cosh k\theta + Z_R' \sinh k\theta} \cdot \frac{g_m E_k Z_i (n-k)}{Z_{ik} + Z_i (n-k)}. \tag{A-7}$$

The values of the input impedances appearing in (A-7) are,

$$Z_{ik} = Z_I' \frac{Z_R' \cosh k\theta + Z_I' \sinh k\theta}{Z_I' \cosh k\theta + Z_R' \sinh k\theta}, \tag{A-8}$$

$$Z_{i(n-k)} = Z_I' \frac{Z_R' \cosh (n-k)\theta + Z_I' \sinh (n-k)\theta}{Z_I' \cosh (n-k)\theta + Z_R' \sinh (n-k)\theta}. \tag{A-9}$$

From (A-7), (A-8) and (A-9),

$$E_{Rk}' = g_m E_k Z_R' \frac{z_I' \cosh (n-k)\theta + z_I'^2 \sinh (n-k)\theta}{2z_I' \cosh n\theta + (1 + z_I'^2) \sinh n\theta}, \tag{A-10}$$

$$E_R'{}_{(n-k)} = g_m E_k Z_R' \frac{z_I' \cosh k\theta + z_I'^2 \sinh k\theta}{2z_I' \cosh n\theta + (1 + z_I'^2) \sinh n\theta} \tag{A-11}$$

The normalized image impedances of the plate and grid channels are the same, so let,

$$z = z_I = z_I'. \tag{A-12}$$

Substitution of the value of E_k from (A-5) in (A-11) gives, if we use (A-12),

$$E_R'{}_{(n-k)} = g_m E_k Z_R' \frac{z^2 \cosh k\theta \cosh (n-k)\theta + z^2 \sinh k\theta \sinh (n-k)\theta + z \sinh n\theta}{[(1 + z^2) \sinh n\theta + 2z \cosh n\theta]^2}. \tag{A-13}$$

The output voltage at the right-hand end of Fig. A-1 is,

$$E_R' = \sum_{k=1}^{n-1} E_R'{}_{(n-k)} = \frac{g_m E_g Z_R' z^2}{[(1 + z^2) \sinh n\theta + 2z \cosh n\theta]^2}$$

$$\times \left\{ \sum_{k=1}^{n-1} \cosh k\theta \cosh (n-k)\,\theta + \mathbf{z}^2 \sum_{k=1}^{n-1} \sinh k\theta \sinh (n-k)\theta \right.$$

$$\left. + \mathbf{z}\,(n-1) \sinh n\theta \right\}$$

$$= \frac{g_m \mathbf{E}_g \mathbf{Z}_R' \mathbf{z}^2 (n-1) \left\{ (1+\mathbf{z}^2) \cosh n\theta + 2\mathbf{z} \sinh n\theta + \dfrac{\sinh (n-1)\,\theta}{(n-1) \sinh \theta} (1-\mathbf{z}^2) \right\}}{2\,[(1+\mathbf{z}^2) \sinh n\theta + 2\mathbf{z} \cosh n\theta]^2}. \tag{A-14}$$

The forward voltage gain normalized to unity when $\mathbf{z} = 1$ is,

$$\mathbf{A}_f = \frac{\mathbf{E}_R'}{g_m \mathbf{Z}_R' \mathbf{E}_g (n-1)/4} = 2\mathbf{z}^2 \frac{[(1+\mathbf{z}^2) \cosh n\theta + 2\mathbf{z} \sinh n\theta] + \dfrac{\sinh (n-1)\,\theta}{(n-1) \sinh \theta} (1-\mathbf{z}^2)}{[(1+\mathbf{z}^2) \sinh n\theta + 2\mathbf{z} \cosh n\theta]^2} \tag{A-15}$$

In similar fashion the normalized backward voltage gain or ratio of the output voltage at the left end of the plate chain in Fig. 3 to the input voltage is,

$$\mathbf{A}_b = 2\mathbf{z}^2 \frac{\dfrac{\sinh (n-1)\,\theta}{(n-1) \sinh \theta} [(1+\mathbf{z}^2) \cosh n\theta + 2\mathbf{z} \sinh n\theta)] + (1-\mathbf{z}^2)}{[(1+\mathbf{z}^2) \sinh n\theta + 2\mathbf{z} \cosh n\theta]^2}. \tag{A-16}$$

APPENDIX B

Effect of the addition of terminating sections

It is often desirable to add unsymmetrical lossless terminating sections to the ends of the filter chains in Fig. 3. In order to find the new general expressions for gain it is necessary to use the expressions below in (B-1) to (B-4).

If an unsymmetrical four-terminal network has image impedances Z_{02} and Z_{01} and propagation constant ϕ and is connected to a generator as shown in Fig. B-1, then,

$$Z_R = Z_{02}\frac{R\cosh\phi + Z_{01}\sinh\phi}{Z_{01}\cosh\phi + R\sinh\phi} = Z_{02}\frac{\cosh\phi + z_{01}\sinh\phi}{z_{01}\cosh\phi + \sinh\phi}. \qquad \text{(B-1)}$$

where

$$z_{01} = \frac{Z_{01}}{R} . z_{02} = \frac{Z_{02}}{R}.$$

Also,

$$E_g = \frac{\sqrt{z_{01}\, z_{02}}\, E}{z_{01}\cosh\phi + \sinh\phi}. \qquad \text{(B-2)}$$

These are the new values for the internal voltage and impedance of the generator driving the chain of identical filter sections.

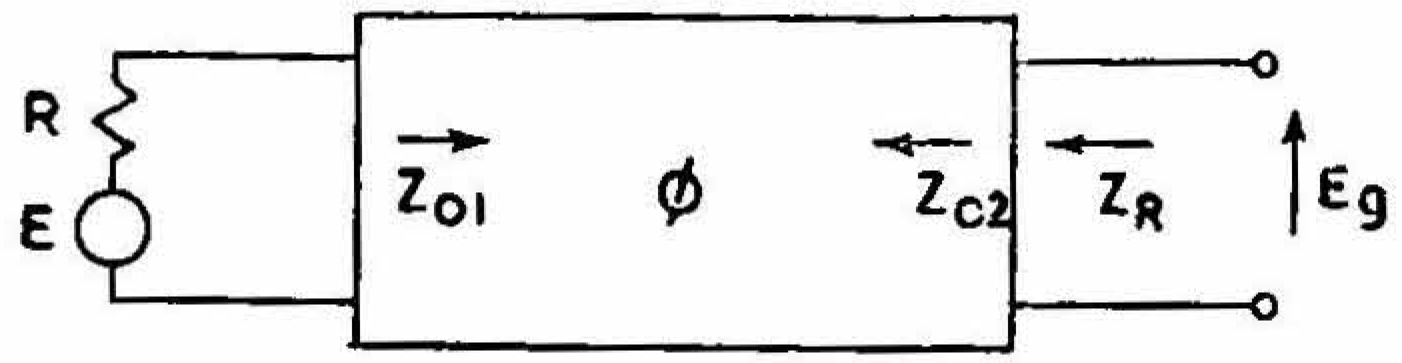

Fig. B-1

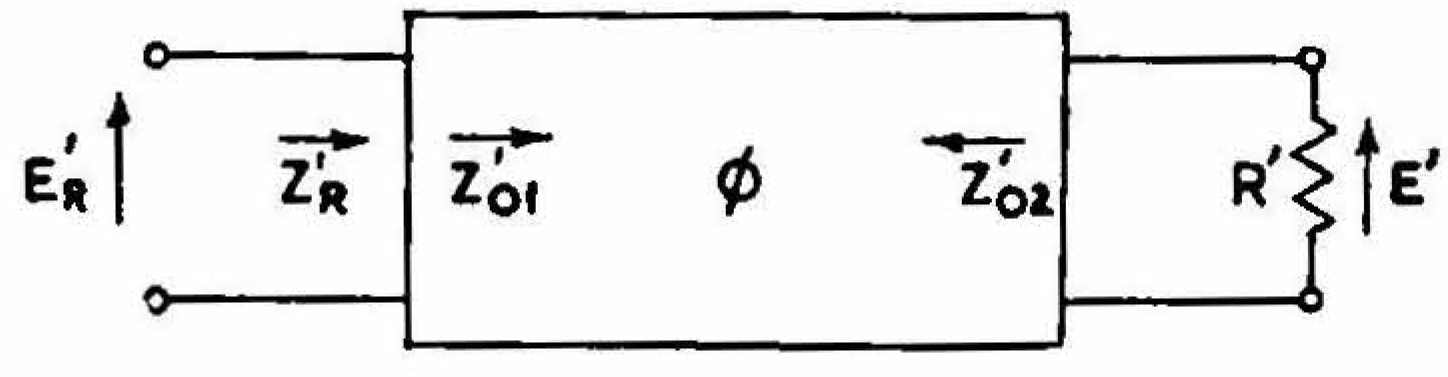

Fig. B-2

Similarly in Fig. B-2,

$$Z_R' = Z_{02}'\frac{\cosh\phi + z_{01}'\sin\phi}{z_{01}'\cosh\phi + \sinh\phi}, \qquad \text{(B-3)}$$

$$E'/E_R' = \frac{\sqrt{\dfrac{z_{01}'}{z_{02}'}}}{\cosh\phi + z_{01}'\sinh\phi}. \qquad \text{(B-4)}$$

In Fig. 4 these unsymmetrical sections have been added to the circuit of Fig. 3, together with two more tubes so that we now have $n + 1$ tubes. Equation (A-15) still holds, except that we now have, if we require $\mathbf{Z}_{02} = \mathbf{Z}_I$, $\mathbf{Z}_{02}' = \mathbf{Z}_I'$,

$$\mathbf{z}_I = \frac{\mathbf{Z}_I}{\mathbf{Z}_R} = \frac{\mathbf{z}_{01}\cosh\phi + \sinh\phi}{\cosh\phi + \mathbf{z}_{01}\sinh\phi}. \tag{B-5}$$

We must also substitute for $\mathbf{E}_g$ the expression given in B-2 to get R in terms of $\mathbf{E}$.

If we require the condition $\mathbf{z}_{01} = \mathbf{z}_{01}'$ then we can write $\mathbf{z}_I = \mathbf{z}_I' = \mathbf{z}$ as before. Equation (A-14) will have the same form as before, except that we sum over $n + 1$ tubes, giving $(n + 1)$ in place of $(n - 1)$ throughout. If we substitute in (B-4) the expression in (B-2) for $\mathbf{E}_g$, the expression from (B-4) for $\mathbf{E}_R$, and the expression in (B-3) for $\mathbf{Z}_R'$ and again normalize the voltage gain $\mathbf{E}'/\mathbf{E}$ to unity, by dividing by $g_m R'(n + 1)/4$ we will get for the new forward gain,

$$\mathbf{A}_f' = \frac{2\mathbf{z}_{01}\mathbf{z}_{02}\mathbf{z}^2\left[(1 + \mathbf{z}^2)\cosh n\theta + 2\mathbf{z}\sinh n\theta\right] + \dfrac{\sinh (n+1)\,\theta}{(n+1)\sinh\theta}(1 - \mathbf{z}^2)}{(\mathbf{z}_{01}\cosh\phi + \sinh\phi)^2\left[(1 + \mathbf{z}^2)\sinh n\theta + 2\mathbf{z}\cosh n\theta\right]^2}, \tag{B-6}$$

Similarly,

$$\mathbf{A}_b' = \frac{2\mathbf{z}_{01}\mathbf{z}_{02}\mathbf{z}^2}{(\mathbf{z}_{01}\cosh\phi + \sinh\phi)^2} \cdot \frac{\dfrac{\sinh (n+1)\,\theta}{(n+1)\sinh\theta}\left[(1+\mathbf{z}^2)\cosh n\theta + 2\mathbf{z}\sinh n\theta\right] + (1 - \mathbf{z}^2)}{\left[(1 + \mathbf{z}^2)\sinh n\theta + 2\mathbf{z}\cosh n\theta\right]^2}. \tag{B-7}$$

In both (B-6) and (B-7) the expression for $\mathbf{z}$ is that given in (B-5).

APPENDIX C

Image Parameters of a Parallel-Tuned Transformer

Consider the tuned transformer[6] of Fig. C-1. The **Z** matrix of the transformer above is,

$$\left[\,\mathbf{Z}\,\right] = j\omega\begin{bmatrix} L_1 & M \\ M & L_2 \end{bmatrix} = j\omega\begin{bmatrix} S_1 & 0 \\ 0 & S_2 \end{bmatrix} + j\omega\begin{bmatrix} L_1 - S_1 & M \\ M & L_2 - S_2 \end{bmatrix}, \tag{C-1}$$

where S_1 and S_2 are arbitrary. They may be chosen so that the transformer represented by the second matrix has a coupling coefficient of unity and a transformation ratio of $a = \sqrt{L_2/L_1}$ if the determinant,

$$\begin{vmatrix} L_1 - S_1, & M \\ M, & L_2 - S_2 \end{vmatrix} = 1, \tag{C-2}$$

and

$$\sqrt{\frac{(L_2 - S_2)}{(L_1 - S_1)}} = \sqrt{\frac{L_2}{L_1}}. \tag{C-3}$$

Solution of these equations given for S_1 and S_2,

$$S_1 = L_1\,(1 - k), \qquad S_2 = L_2\,(1 - k). \tag{C-4}$$

The equivalent circuit for the transformer as determined by (C-1) and (C-4) is the series combination of two self-inductances and the transformer with unity coupling in Fig. C-2 (*a*), which is in turn equivalent to the circuit with an ideal transformer of Fig. C-2 (*b*).

The complete circuit of Fig. C-1 may be drawn as shown in Fig. C-3 (*a*) and (*b*), where the ideal transformer has been moved to the left, and proper impedance changes made.

Because the transformer is now symmetrical, if we assume identical tune frequencies $\omega_0 = 1/\sqrt{L_1C_2} = 1/\sqrt{L_2C_2}$, the open and short circuit impedances may be obtained for a half-section, giving:

$$\mathbf{Z}_{0c}' = \frac{j\,(1 + k)\,x}{\omega_1 C_2\,[1 - (1 + k)\,x^2]}, \quad \mathbf{Z}_{sc}' = \frac{j\,(1 - k)\,x}{\omega_0 C_2\,[1 - (1 - k)\,x^2]} \tag{C-5}$$

where $x = \omega/\omega_0$.

From these impedances, by Bartlett's Bisection Theorem,

$$\mathbf{Z}_I = \sqrt{\mathbf{Z}_{0c}'\mathbf{Z}_{sc}'} = \frac{x}{\omega_1 C_2}\sqrt{\frac{(1 - k^2)}{2x^2 - 1 - x^4\,(1 - k^2)}}, \tag{C-6}$$

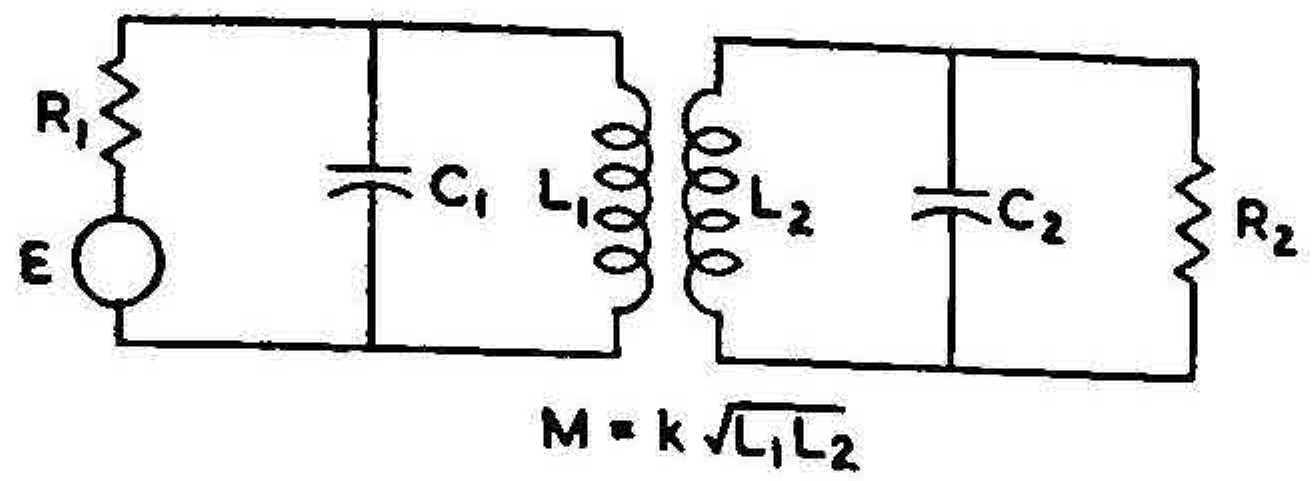

Fig. C-1

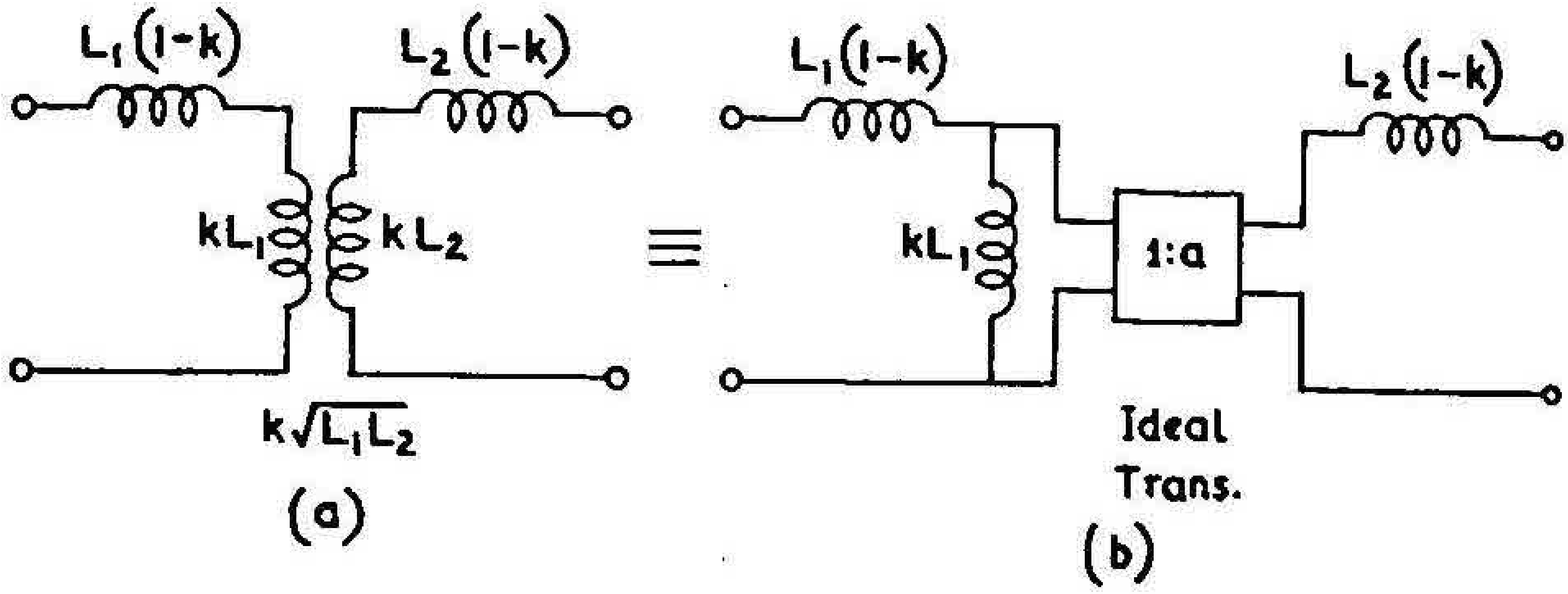

Fig. C-2

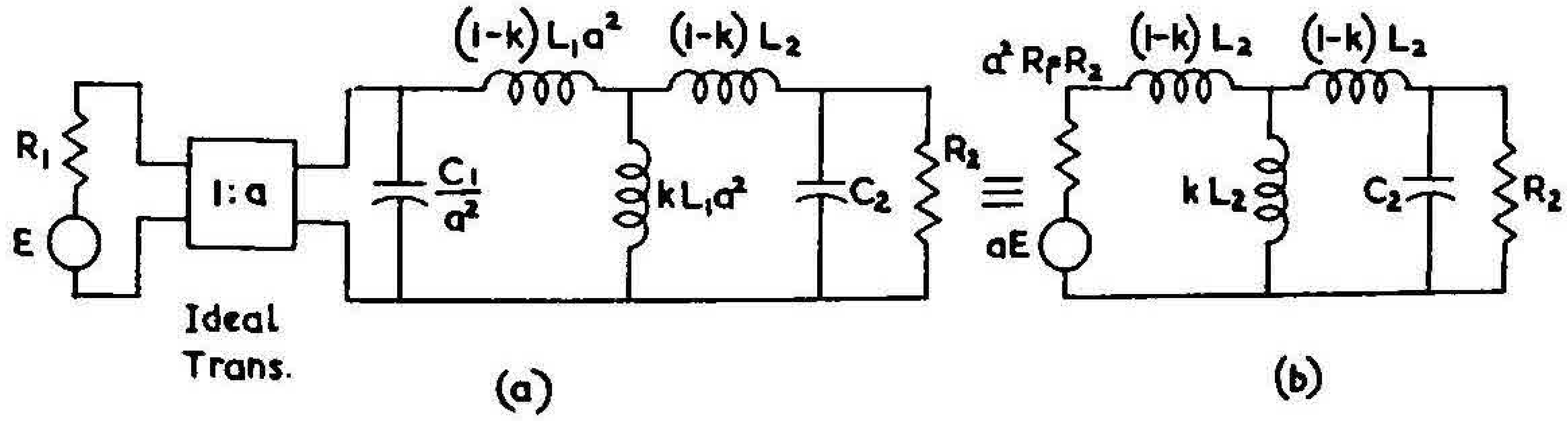

Fig. C-3

and

$$\tanh\frac{\theta}{2} = \sqrt{\frac{Z_{sc}'}{Z_{0c}'}} = \sqrt{\frac{1-k}{1+k}} \cdot \sqrt{\frac{1-(1+k)\,x^2}{1-(1-k)\,x^2}}. \tag{C-7}$$

The cut-off frequencies, from C-7, are at,

$$\omega_1 = \frac{\omega_0}{\sqrt{1+k}}, \qquad \omega_2 = \frac{\omega_0}{\sqrt{1-k}}. \tag{C-8}$$

The minimum value of Z , obtained by setting the derivative of C-6 to zero is at,

$$\omega_m = \frac{\omega_0}{\sqrt{1-k^2}} = \sqrt{\omega_1\omega_2}. \tag{C-9}$$

The bandwidth, $\Delta\omega \equiv \omega_2 - \omega_1$ is from C-8 and C-9,

$$\Delta\omega = \frac{\omega_m}{\sqrt{1-k^2}}\left(\sqrt{1+k} - \sqrt{1-k}\right). \tag{C-10}$$

The value of Z_t at the geometrical mid-band, $\omega = \omega_n$ is from (C-6), (C-9) and (C-10),

$$Z\,(\min) = \frac{\sqrt{1-k^2}}{\omega_0 C_2(\sqrt{1+k} - \sqrt{1-k})} = \frac{1}{\Delta\omega C_2}. \tag{C-11}$$

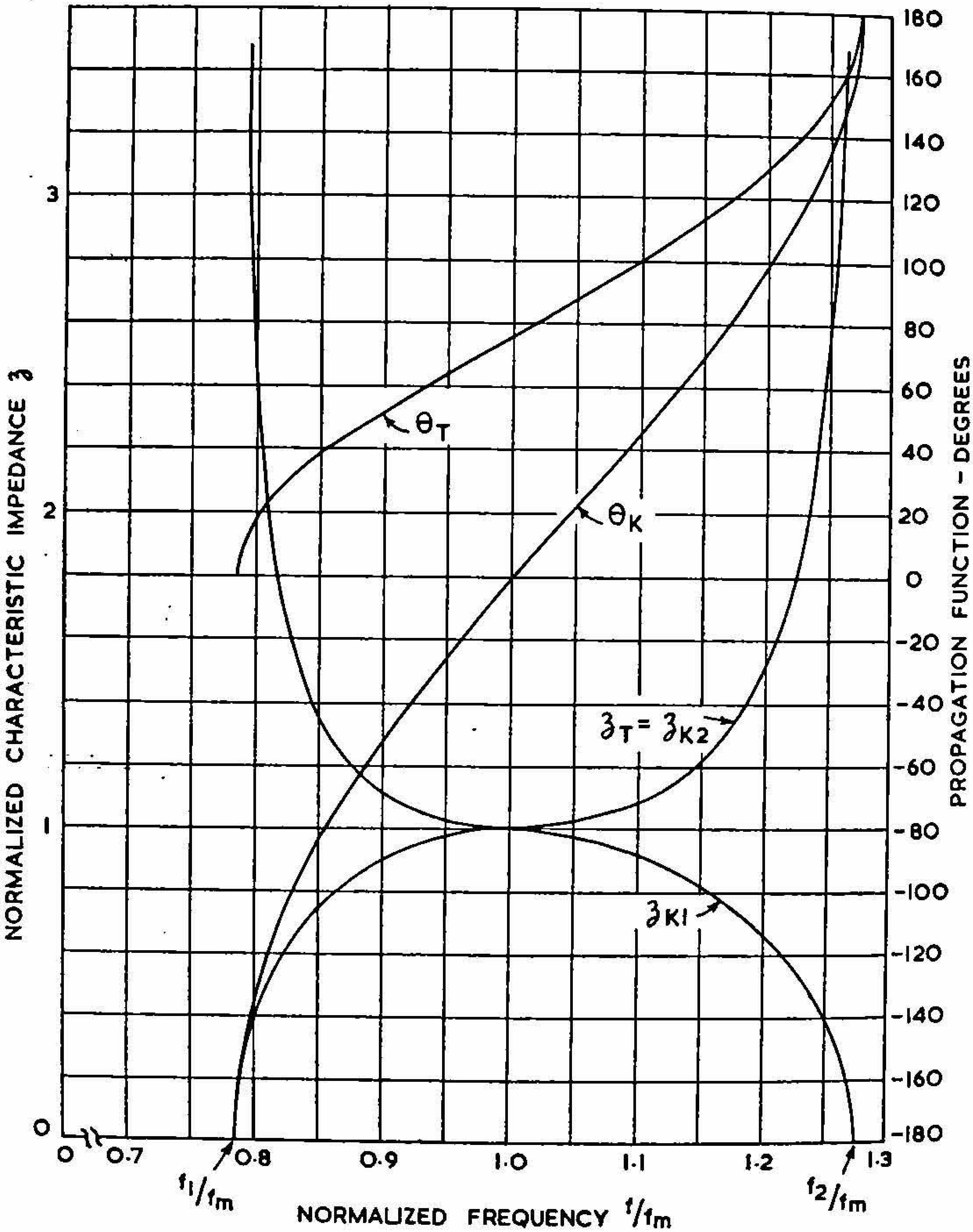

FIG. C-4. Normalized characteristic impedance of a parallel-tuned transformer (z_T) and of a constant-k filter (z_{K1} mid-shunt, and z_{K1}, mid-series), and propagation functions (θ_T and θ_K) plotted against frequency.

If Z_t is normalized with respect to this value, it may be shown that:

$$\mathbf{z} = \frac{1}{\sqrt{1 - \left(\frac{\omega_m}{\Delta\omega}\right)^2 \left(\frac{\omega}{\omega_m} - \frac{\omega_m}{\omega}\right)^2}}. \tag{C-12}$$

This is the same as the mid-shunt impedance of a constant-*k* type band-pass filter.

The propagation function is from (C-7), (C-8) and (C-9),

$$\sinh \theta = \frac{2j}{\omega_2^2 - \omega_1^2} \sqrt{(\omega - \omega_1^2)(\omega_2^2 - \omega^2)}\,, \tag{C-13}$$

This is *not* the same as that of a full section of a constant-*k* band-pass filter, which is,

$$\sinh \theta = 2j\left(\frac{\omega_m}{\Delta\omega}\right)\left(\frac{\omega}{\omega_m} - \frac{\omega_m}{\omega}\right)\sqrt{1 - \left(\frac{\omega_m}{\Delta\omega}\right)^2\left(\frac{\omega}{\omega_m} - \frac{\omega_m}{\omega}\right)^2}. \tag{C-14}$$

In Fig. C-4 the normalized characteristic impedances and propagation constants are plotted for the parallel-tuned transformer and the constant-*k* band-pass filter for a bandwidth corresponding to $k = 0{\cdot}45$ for the transformer.

If a single transformer is used, the response will be maximally flat if loaded with resistances across the tuning capacitances given in each case by,

$$R = \frac{1}{\Delta\omega C}. \tag{C-15}$$

A perfect match will result at midband ($\omega = \omega_m$) under these conditions.

APPENDIX D

Design Parameters of a Series-Parallel Tuned Transformer Based on Simple Filter Theory

The Z matrix for the transformer[9, 10] in Fig. D-1 may be split up so as to give a series inductance on only one side and a transformer with unity coupling, as follows:

$$\left[Z \right] = j\omega \begin{bmatrix} L_1 & M \\ M & L_2 \end{bmatrix} = j\omega \begin{bmatrix} L_1(1-k^2) & O \\ O & O \end{bmatrix} + j\omega \begin{bmatrix} k^2L_1 & M \\ M & L_2 \end{bmatrix}. \tag{D-1}$$

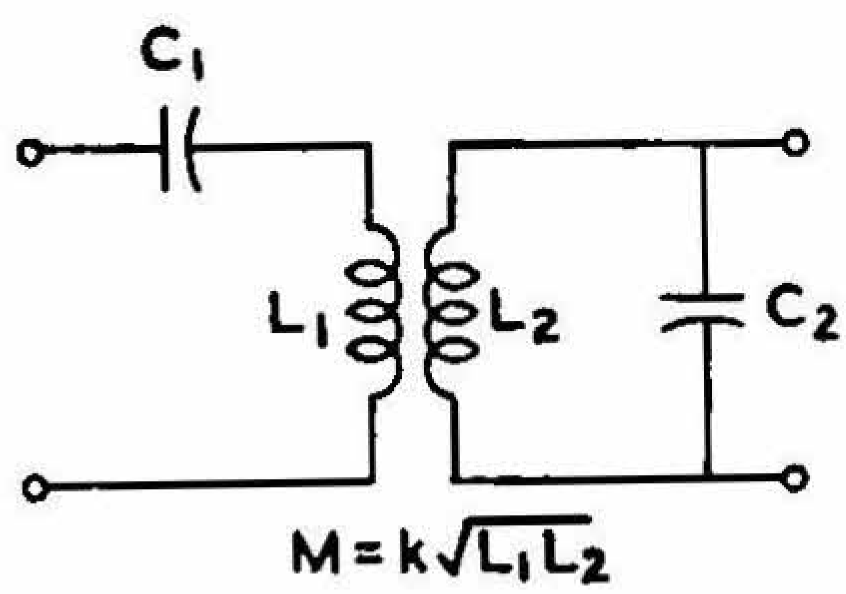

Fig. D-1

The transformer represented by the second matrix has a transformation ratio $\frac{a}{k} = \frac{1}{k}\sqrt{\frac{L_2}{L_1}}$. It may be replaced by an ideal transformer with this transformation ratio and a parallel inductor, as shown in Fig. D-2 (*a*).

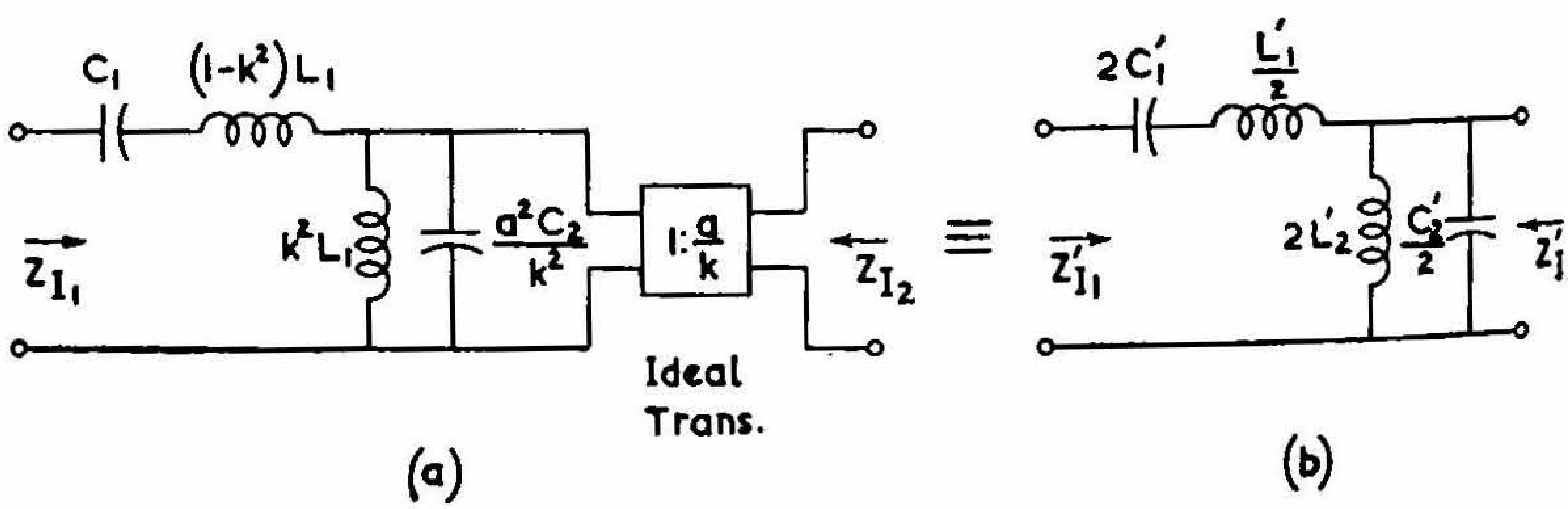

FIG. D-2

(Capacitance C_2 has been moved through the ideal transformer).

The equivalent circuit for the transformer shown in Fig. D-2 (*b*) has the form of a simple band-pass constant-*k* filter half-section. It will be a constant-*k* half-section if $L_1'/C_2' = L_2'/C_1' = R^2$, and reactive parameters may be expressed in terms of the tune frequency $\omega_0 = 1/\sqrt{L_1'C_1'} = 1/\sqrt{L_2'C_2'}$ and the bandwidth $\Delta\omega = \omega_2 - \omega_1$ between upper and lower cut-off frequencies.

$$\frac{L_1'}{2} = \frac{R}{\Delta\omega},$$

$$2C_1' = \frac{\Delta\omega}{R\omega_m^{\,2}},$$

$$\frac{C_2'}{2} = \frac{1}{R\Delta\omega},$$

$$2L_2' = \frac{R\Delta\omega}{\omega_m^{\,2}}. \tag{D-2}$$

If we equate the reactances in Fig. D-2 (*a*) to the same quantities and solve for L_1, C_1, etc. in terms of R_1 and $R_2 = a^2R_2/k^2$ we get,

$$C_1 = \frac{\Delta\omega}{R_1\omega_m^{\,2}}, \qquad k = \frac{\dfrac{\Delta\omega}{\omega_2}}{\sqrt{1+\left(\dfrac{\Delta\omega}{\omega_m}\right)^2}},$$

$$L_1 = \left[1+\left(\frac{\Delta\omega}{\omega_m}\right)^2\right]\frac{R_1}{\Delta\omega}, \qquad \omega_1\omega_2 = \omega_m^{\,2},$$

$$C_2 = \frac{1}{\Delta\omega R_2}, \qquad \omega_1 = \sqrt{\omega_m^{\,2}+\left(\frac{\Delta\omega}{2}\right)^2} - \frac{\Delta\omega}{2},$$

$$L_2 = \frac{R_2\Delta\omega}{\omega_m^{\,2}}, \qquad \omega_2 = \sqrt{\omega_m^{\,2}+\left(\frac{\Delta\omega}{2}\right)^2} + \frac{\Delta\omega}{2}. \tag{D-3}$$

If terminated in R_1 and R_2, this transformer will have a maximally flat transmission band with 1 *db* points at ω_1 and ω_2.

The image impedances are,

$$Z_{I1} = R_1\sqrt{1-\left(\frac{\omega_m}{\Delta\omega}\right)^2\left(y-\frac{1}{y}\right)^2},$$

$$Z_{I2} = R_2\sqrt{1-\left(\frac{\omega_m}{\Delta\omega}\right)^2\left(y-\frac{1}{y}\right)^2}. \tag{D-4}$$

where $y = \omega/\omega_m$.

The propagation function is the same as for a half-section of a constant-*k* filter or just half of that shown in Fig. C-4. The normalised characteristic impedances are those plotted there.